Case Studies in Engineering Failure Analysis 7 (2016) 24–31

Contents lists available at ScienceDirect

Case Studies in Engineering Failure Analysis

journal homepage: www.elsevier.com/locate/csefa

Case study

Failure analysis of a diesel generator connecting rod

C. Juarez [a], F. Rumiche [a,*], A. Rozas [a], J. Cuisano [b], P. Lean [b]

[a] CITE Materiales, Pontificia Universidad Católica del Perú, Lima, Peru
[b] Mechanical Engineering Department, Pontificia Universidad Católica del Perú, Lima, Peru

ARTICLE INFO

Article history:
Received 6 May 2016
Received in revised form 7 June 2016
Accepted 10 June 2016
Available online 18 June 2016

Keywords:
Connecting rod
Fatigue
Fracture
Diesel engine
Manufacturing defects

ABSTRACT

This paper presents the results of a failure analysis investigation conducted in a connecting rod from a diesel engine used in the generation of electrical energy. The investigation included an extensive analysis of the con-rod material as well as the fracture zone. The investigation involved the following experimental procedures and testing techniques: visual inspection, fractography, magnetic particle inspection, chemical analysis, tensile and hardness testing, metallography, and microanalysis. The connecting rod was fabricated from an AISI/SAE 4140 low alloy steel; chemical composition, mechanical properties and microstructure were appropriate for the application. The connecting rod fractured at the body in a section close to the head; the origin of the fracture was located at the con-rod lubrication channel. The lubrication channel exhibited an area containing a tungsten based material, presumably from a machining tool, embedded in its surface as a result of a deficient manufacturing process. This area acted as nucleation site for cracks that propagate through the connecting rod section by a fatigue mechanism, reducing its section and finally producing its catastrophic failure.
© 2016 The Authors. Published by Elsevier Ltd. This is an open access article under the CC BY-NC-ND license (http://creativecommons.org/licenses/by-nc-nd/4.0/).

1. Background

Connecting rods are mechanical components that convert the piston alternative motion in the crankshaft rotational motion. They are subjected to a complex state of stresses which includes compression stresses associated to the pressure exerted by the combustion gases, and tensile stresses related to the inertia of the components in motion, either alternative or rotational [1,2]. Failures in con-rods have been reported in the literature, being associated to fatigue, overload bending, bearing failure, improperly adjusted bolts, spalling, and assembly deficiencies [3–9].

This paper presents the results of a failure analysis investigation conducted in a connecting rod from a diesel engine (18 V, four-stroke) used in the generation of electrical energy. The continuous output of the engine was 10.5 MW, at 600 rpm; before the failure of the con-rod it accumulated 35836 service hours, working with a load factor of 80%. The connecting rod (total length: 1463 mm, weight: 134 kg) had a drilled channel along its body, through which pressured lubrication oil was transported to the piston pin. Fig. 1 shows the failed con-rod, which fractured in the body section, close to the head.

* Corresponding author. Tel.: +51 6262000x4892.
E-mail address: frumiche@pucp.edu.pe (F. Rumiche).

http://dx.doi.org/10.1016/j.csefa.2016.06.001
2213-2902/© 2016 The Authors. Published by Elsevier Ltd. This is an open access article under the CC BY-NC-ND license (http://creativecommons.org/licenses/by-nc-nd/4.0/).

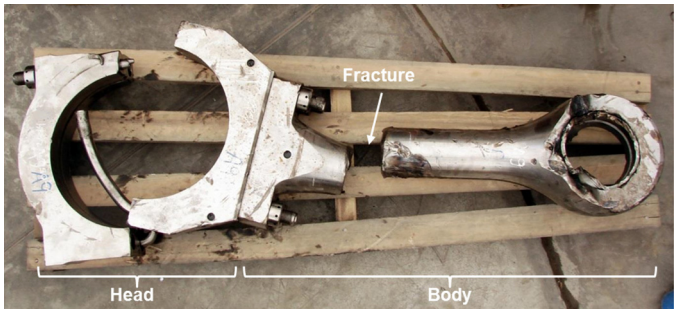

Fig. 1. Failed connecting rod.

2. Experimental procedures

The first stage of the analysis was the visual inspection of the connecting rod and the analysis of the fracture surface. Then, a comprehensive characterization of the con-rod material was conducted; samples were removed from a zone away from the fracture zone (Fig. 2 shows the location of samples for the tests, as well as the dimensions of the con-rod) in order to carry out the following tests: chemical analysis, hardness test, metallographic analysis, and tensile test. Chemical analysis was conducted with a Bruker Magellan Q8 atomic emission spectrometer, according to ASTM E415-14 [10]. Tensile tests were conducted in longitudinal samples (2) located at the mid radio of the body of the con-rod, tests were conducted according to ASTM A370-15 standard [11] using a Zwick Roell Z250 tensile test machine. Hardness testing was conducted according to ASTM E384-11e1 standard [9] employing a Zwick Roell ZHV30 hardness tester (9 indentations). Samples for metallographic analysis were prepared according to ASTM E3-11 [12] and ASTM E407-07(2015)e1 [13] standards, they were mounted in epoxy resin and subjected to a grinding and polishing processes with sand paper and diamond paste, respectively. Samples microstructure was revealed after chemical etching with a 2% Nital solution; the analysis was carried out with a Leica M2 optical microscope, equipped with a digital camera.

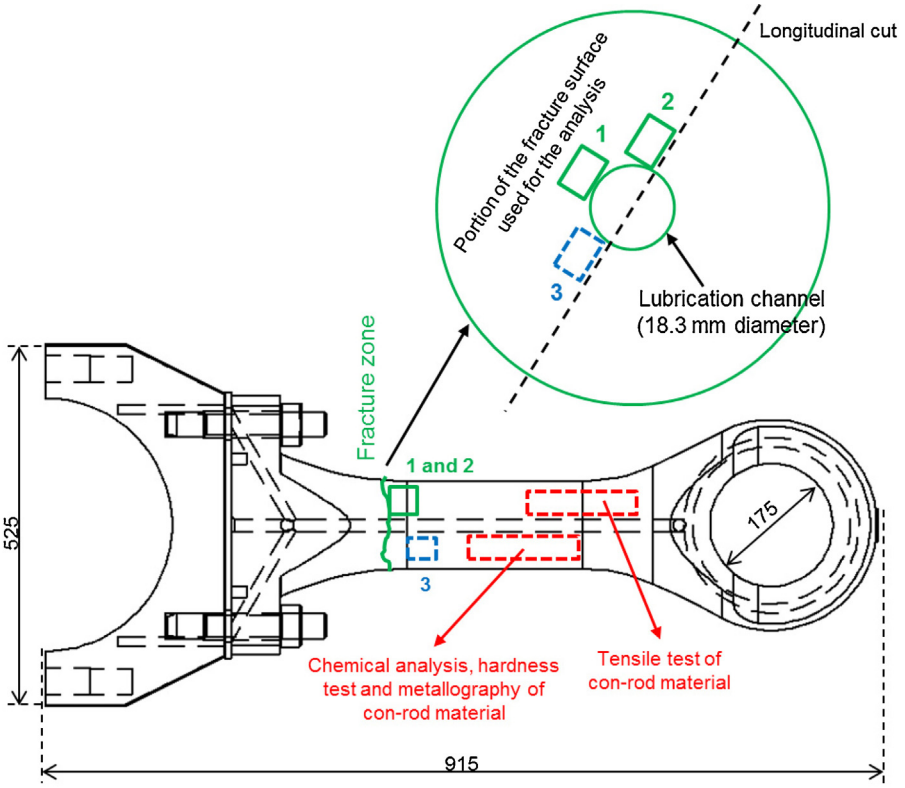

Fig. 2. Location of samples for the analysis of the con-rod material and the fracture zone.

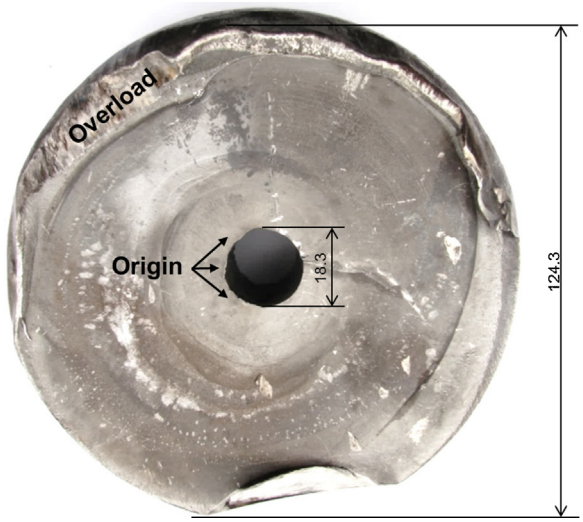

Fig. 3. Fracture surface of the connecting rod.

A comprehensive analysis of the fracture zone was also performed. Magnetic particle inspection, metallographic analysis and hardness testing, as well as microanalysis, were conducted in samples obtained from the fracture origin site. A longitudinal cut through the lubrication channel (since this was the zone were cracking started, as explained below) was carried out in order to obtain the samples for the analysis, Fig. 2 also shows the location of samples used for the evaluation, lubrication channel diameter was 18.3 mm. Samples 1 and 2 were removed from the fracture surface area, whereas sample 3 was removed from an area away from it. Metallography and hardness tests were carried out as described above. Magnetic particle testing was performed according to ASTM E709-15 standard [14], alternating current magnetic field generated with a Magnaflux Magnetic Yoke, and fluorescent particles, were used. A FEI Quanta 650 scanning electron microscope, operating at 30 kV, equipped with an EDAX energy dispersive spectrometer, was employed for microanalysis of the samples.

3. Results and discussion

3.1. Visual inspection and fractography

Fig. 3 shows the fracture surface of the connecting rod. The con-rod fractured in the body through a section perpendicular to its axis, close to the head. Previous investigations reveal that connecting rods are prone to fail in this area, since the highest deformation and level of stresses, according to finite element simulations, occur in this location [15,16]. A fatigue pattern with beach marks was observed; fatigue cracking initiates in multiple sites at the lubrication channel, as seen in Fig. 3(a), and propagates to the external part of the con-rod. Fatigued area covers more than 75% of the connecting rod section, suggesting low magnitude nominal stresses; the rest of the fracture pattern exhibits an overload pattern, as shown also in Fig. 3.

Although a fatigue fracture is typical in cases of failure of connecting rods, the observed pattern (i.e. from the center to the exterior), is not common. Therefore, the analysis at the fracture zone was focused on the origin of the fracture (i.e. the lubrication channel).

3.2. Connecting rod material properties

Table 1 shows the results of the chemical analysis of the material of the connecting rod. The composition corresponds to that for a low alloy medium carbon steel, compatible to the AISI/SAE 4140 steel [17], with a small addition of Ni.

Results from tensile test are shown in Table 2. The average tensile and yield strength values are 855 and 659 MPa, respectively. The average elastic modulus and elongation values are 201 MPa and 20%, correspondingly.

Table 1
Chemical composition of the connecting rod material.

Element	C	Mn	Si	Cr	Mo	Ni	Cu	P	S
wt.%	0.48	0.56	0.33	1.02	0.24	0.25	0.08	0.010	0.015

Table 2
Tensile properties of the connecting rod material.

Yield strength (MPa)	659
Tensile strength (MPa)	855
Elastic modulus (GPa)	201
Elongation (%)	20

Table 3
Hardness of the connecting rod material.

Indentation	1	2	3	4	5	6	7	8	9
HV0.5	273	279	277	270	279	281	269	278	279

Table 3 shows the results of the hardness test. The obtained average hardness value was 276 VH. The metallographic analysis of the con-rod material revealed a tempered martensite microstructure, as observed in Fig. 4. The values of the properties and the microstructure are consistent with those reported for an AISI/SAE 4140 steel in the quenched and tempered state [17], and are appropriate for an application as a connecting rod.

3.3. Fracture zone analysis

Fig. 5 shows an image of the longitudinal cut through the lubrication channel at the fracture zone. Very coarse machining marks as well as an area that exhibit loss of material were identified in the channel. Magnetic particle examination revealed

Fig. 4. Microstructure of the connecting rod material.

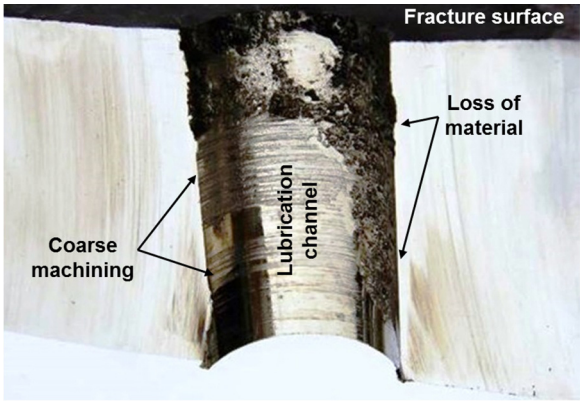

Fig. 5. View of the lubrication channel at the fracture zone.

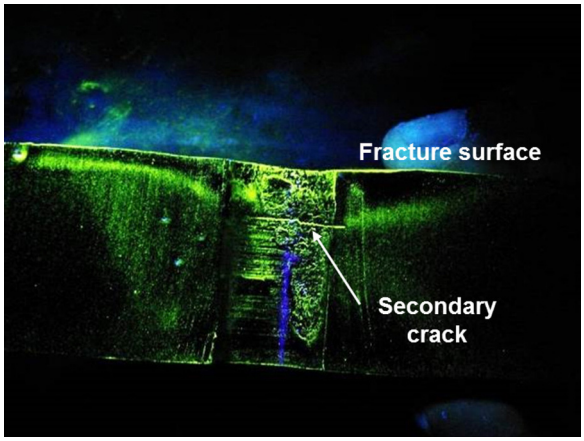

Fig. 6. Secondary crack revealed by magnetic particle inspection.

the presence of secondary cracks parallel to the fracture surface, as observed in Fig. 6. It is clear that cracks propagate from the lubrication channel to the exterior surface of the connecting rod, as indicated for one secondary crack (white arrow) in the figure.

Metallographic samples examination (samples 1 and 2) revealed the presence of a white layer (as observed in the micrographs) in the surface of the lubrication channel, where cracks nucleate, as observed in Fig. 7(a). Cracks propagate toward the exterior of the con-rod, as seen in Fig. 7(b). The white layer exhibits a wide-ranging thickness, Fig. 7(a) shows two thickness measurements: 106.28 and 83.78 μm. In addition, a heat affected zone with a varied size was identified; Fig. 7(a) also shows two measurements: 196.35 and 168.08 μm.

An analysis of sample 3, away from the fracture zone, do not show evidence of the white layer or the heat affected zone. However, a coarse machining finishing of the channel is observed in these areas, as shown in Fig. 8.

Fig. 9 presents the hardness test indentations (1–6) of the lubrication channel sample at the fracture zone, the inset shows a close up view of the indentations 1–3. Table 4 presents the results of the test. The white layer exhibits an extremely high hardness value, of approximately 1000 HV (indentations 1 and 4), which is not possible to attain with an AISI/SAE 4140 steel. Therefore, it is evident that the white layer is composed of a material that has been embedded in the steel matrix. The presence of a heat affected zone (indentations 2 and 5), with a hardness value of up to 408 HV, indicates that the process to embed this material in the steel involved high temperatures.

The microanalysis revealed the composition of the white layer. As observed in Fig. 10, which shows the superimposing of two energy dispersive spectra (i.e. the white layer (red line) and the rod material (black line)), the white layer contains a high amount of tungsten (W). This is confirmed with a line scan test, performed from the internal part of the rod to the white

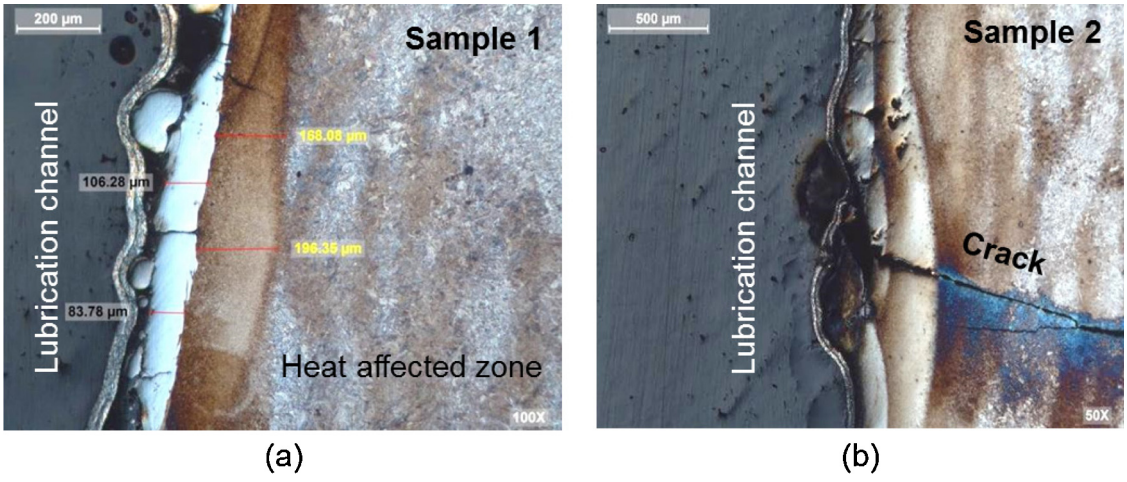

Fig. 7. Micrographs of the microstructure at the lubrication channel, sample 1 (a) and sample 2 (b).

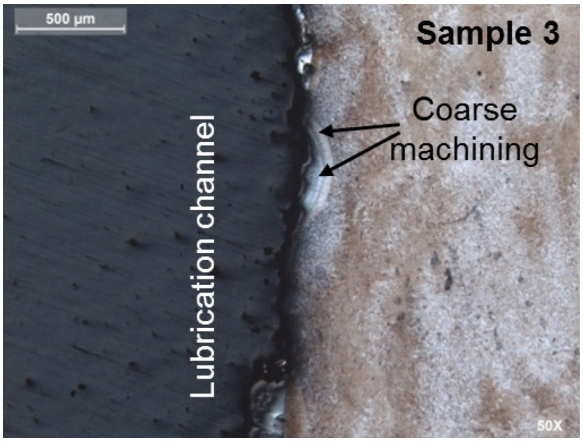

Fig. 8. Micrograph of the microstructure at the lubrication channel in sample 3.

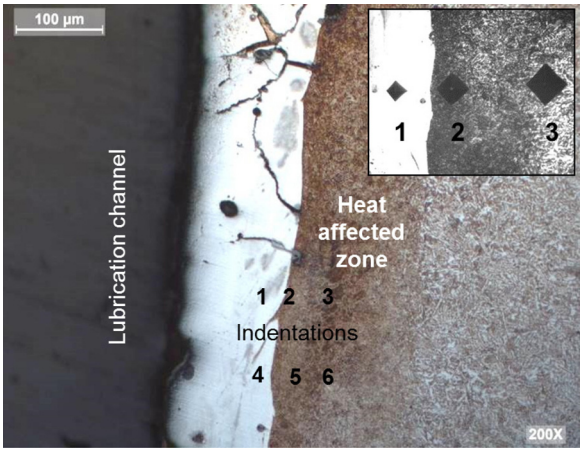

Fig. 9. Hardness test indentations (1–6) in the fracture zone.

layer; as observed in Fig. 11 the content of W increases dramatically right at the interface between the heat affected zone and the white layer.

The presence of tungsten and the evidence of exposure to temperatures high enough to promote its embedding in the steel substrate and the formation of a heat affected zone, are compatible with the process of electrical discharge machining (EDM). In EDM an electrically conductive material is machined by producing a controlled and localized electric spark between an electrode and a workpiece [18]. Temperatures involved in this process could reach values up to 12,000 °C and tungsten based materials are used as electrodes. Therefore, it could be presumed that EDM was used to machine the lubrication channel and that the embedding of W and the formation of the corresponding heat affected zone were produced as a result of its deficient application.

Based on all the findings a sequence of events is proposed: an overheating event during the machining of the lubrication channel produced the melting or plasticization of the tungsten based tool, which in turn, and assisted by the mechanical pressure exerted, has resulted in an embedded piece of W in the channel, generating a stress concentration area, where multiple cracks have nucleated. The cracks have growth and propagated by a fatigue mechanism, reducing the section of the con-rod until the remaining section was not able to withstand the stresses, producing the catastrophic rupture of the connecting rod.

Table 4
Hardness values for the indentations at the fracture zone.

Indentation	1	2	3	4	5	6
HV0.5	936	408	254	1081	367	256

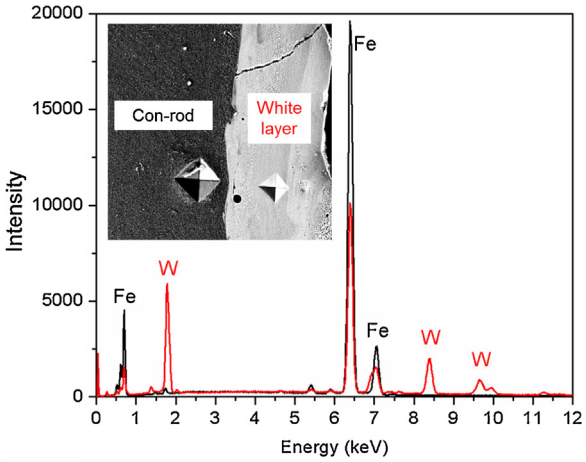

Fig. 10. Energy dispersive spectroscopy spectra for white layer and rod material. (For interpretation of the references to color in this figure citation, the reader is referred to the web version of this article.)

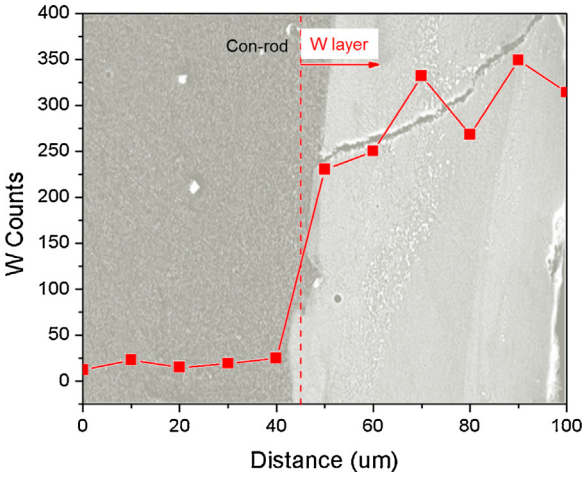

Fig. 11. W content variation from con-rod material to W layer.

4. Conclusions

The connecting rod was fabricated from a AISI/SAE 4140 low alloy steel. Chemical composition, mechanical properties and microstructure are adequate for the application. Failure occurred at the body of the con-rod, close to the head, and involved the propagation by a fatigue mechanism of cracks nucleated at the lubrication channel. A layer of a tungsten based material embedded in a portion of the lubrication channel served as the area for crack nucleation. The W layer was possibly generated during the connecting rod fabrication process, particularly, during the lubrication channel machining.

References

[1] Heywood J. Internal combustion engine fundamentals. McGraw-Hill Education: 1st ed.; 1998.
[2] Shenoy P. Dynamic load analysis and optimization of connecting rod (M.S. thesis). The University of Toledo; 2004.
[3] Ilman M, Barizy R. Failure analysis and fatigue performance evaluation of a failed connecting rod of reciprocating air compressor. Eng Failure Anal 2015;56:142–9.
[4] Lei Xu X, Wei Yu Z. Failure analysis of a diesel engine connecting rod. J Failure Anal Prev 2007;7:316–20.
[5] Clevite engine bearings: engine bearing failure analysis guide, clevite 77, form CL77-3-402; 2002.
[6] Afzal A. Fatigue behavior and life predictions of forged steel and powder metal connecting rods (M.S. thesis). The University of Toledo; 2004.
[7] Rabb R. Fatigue failure of a connecting rod. Eng Failure Anal 1996;3:13–28.
[8] Kohler engines: failure analysis guidebook, form TP-2298-B; 2002.
[9] Khare S, Singh O, Bapanna K, Sasun C. Spalling investigation of connecting rod. Eng Failure Anal 2012;19:77–86.
[10] ASTM E415-15 standard test method for analysis of carbon and low-alloy steel by spark atomic emission spectrometry. West Conshohocken, PA: ASTM International; 2015.
[11] ASTM A370-15 standard test methods and definitions for mechanical testing of steel products. West Conshohocken, PA: ASTM International; 2015.

[12] ASTM E3-11 standard guide for preparation of metallographic specimens. West Conshohocken, PA: ASTM International; 2011.
[13] ASTM E407-07(2015) e1 standard practice for microetching metals and alloys. West Conshohocken, PA: ASTM International; 2015.
[14] ASTM E709-15 standard guide for magnetic particle testing. West Conshohocken, PA: ASTM International; 2015.
[15] Samal P, Murali B, Abhilash, Pasha T. Finite element analysis of connecting rod of IC engine. MATEC Web Conf 2015;34:02004.
[16] Chikalthankar S, Nandedkar V, Prasad S. Fatigue numerical analysis for connecting rod. Int J Eng Res Appl 2012;2:628–32.
[17] ASM Handbook. Properties and selection: irons steels and high-performance alloys, vol. 1. ASM International; 1990.
[18] Jameson E. Electrical discharge machining. Society of Manufacturing Engineers; 2001.